

# Analysis of plane frame structure using base force element method

Yijiang Peng\*, Yaqiong Bai and Qing Guo

Key Laboratory of Urban Security and Disaster Engineering, Ministry of Education, Beijing University of Technology, Beijing, 100124, China

(Received July 23, 2016, Revised October 31, 2016, Accepted November 1, 2016)

**Abstract.** The base force element method (BFEM) is a new finite element method. In this paper, a degenerated 4-mid-node plane element from concave polygonal element of BFEM was proposed. The performance of this quadrilateral element with 4 mid-edge nodes in the BFEM on complementary energy principle is studied. Four examples of linear elastic analysis for plane frame structure are presented. The influence of aspect ratio of the element is analyzed. The feasibility of the 4 mid-edge node element model of BFEM on complementary energy principles researched for plane frame problems. The results using the BFEM are compared with corresponding analytical solutions and those obtained from the standard displacement finite element method. It is revealed that the BFEM has better performance compared to the displacement model in the case of large aspect ratio.

**Keywords:** base force element method; complementary energy principle; plane frame; aspect ratio; finite element method

## 1. Introduction

The finite element method (FEM) which is an important branch of computational mechanics has been broadly adopted in scientific research and engineering applications. But with the continuous development of scientific research and engineering applications, the conventional finite element method also shows some obvious deficiencies. For decades, many researchers make great efforts in developing novel principles, techniques, algorithms, and schemes to improve precision, efficiency, robustness, and applicability of the conventional FEM.

Various finite element models have been proposed and they are robust and insensitive to mesh distortion, such as the equilibrium models (Veubeke 1965, 1972), the hybrid stress method (Pian 1964, Pian and Chen 1982, Pian and Sumihara 1984, Zhang *et al.* 2007), the integrated force method (Patnaik 1973, 1986, Patnaik *et al.* 1991), the mixed approach (Zienkiewicz 1979), the new natural coordinate methods (Long *et al.* 1999, Long *et al.* 2009, Long *et al.* 1999, Long *et al.* 2010), the smoothed finite element method (Liu *et al.* 2007), the incompatible displacement modes (Wilson *et al.* 1973), the assumed strain method (Simo and Hughes 1986), the enhanced strain modes (Piltner and Taylor 1995), the selectively reduced integration scheme (Hughes 1980), the quasi-conforming element method (Tang *et al.* 1984), the generalized conforming method (Long and Huang 1988), the Alpha finite element method (Liu *et al.* 2008), the unsymmetric method (Rajendran and Liew 2003), the new spline finite

element method (Chen *et al.* 2010), the extended finite element method (Moes *et al.* 1999) and so on.

In recent years, some scholars still adhere to explore the finite element method based on complementary energy principle (Cen *et al.* 2011, Fu *et al.* 2010, Cen *et al.* 2011, Cen *et al.* 2011, Santos and Almeida 2010, Santos 2011, Santos and Paulo 2011, Darilmaz 2005). A family of arbitrarily shaped elements (Santos and Moitinho de Almeida 2014) is derived which takes advantage of the special structure of the framework for the development of hybrid stress finite elements. The key feature is to explicitly approximate, in the parent domain, either the second Piola-Kirchhoff, the first Piola-Kirchhoff, or the Cauchy stresses, and to enforce the divergence-free condition in the physical domain using their corresponding first Piola-Kirchhoff projections. The development of a novel updated Lagrangian variational formulation (Santos 2016) and its associated finite element model were addressed for the geometrically nonlinear quasi-static analysis of cantilever beams. The formulation is based on an incremental complementary energy principle. The proposed finite element model only contains nodal bending moments as degrees of freedom. The model is used for the analysis of problems modeled by the so-called elastica theory.

In recent years, the new finite element method-BFEM which is described by "base forces" given by Gao (2003) has been greatly developed. Using the concept of base forces as state variables, a three-dimensional formulation of base force element method (BFEM) on complementary energy principle was proposed by Peng and Liu (2009) for geometrically nonlinear problems. And the new finite element method based on the concept of base forces was called as the Base Force Element Method (BFEM) by Peng and Liu. In the paper (Peng *et al.* 2014a), a 2D base force base force element method with complementary energy

\*Corresponding author, Professor  
E-mail: pengyijiang@bjut.edu.cn

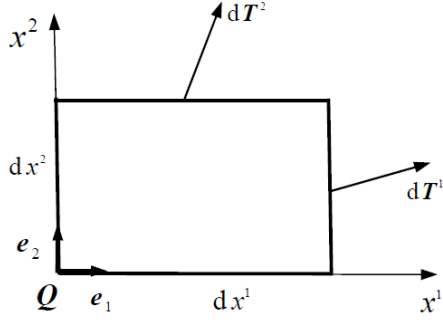


Fig. 1 Base forces on planar problem

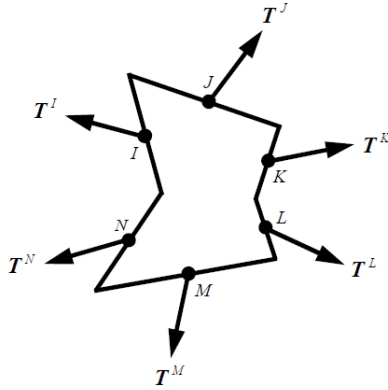


Fig. 2 A concave polygonal element with mid-edge nodes

principle for arbitrary meshes was researched, and its computational performance was studied. Large-scale computing element model on complementary energy was proposed by Peng *et al.* (2015) for rock engineering problems. The base force element method (BFEM) on the potential energy principle was researched by Peng *et al.* (2011) in which the stiffness matrix to the plane problems of elasticity was expressed by four-side plane element and the polygonal element.

In the present paper, a degenerated 4-mid-node plane element from concave polygonal element of BFEM was proposed. The quadrilateral element model with 4 mid-edge nodes in the BFEM on complementary energy principle is applied to the analysis of plane frame structure. The performance of the 4 mid-edge node model of BFEM will be researched and be compared to the displacement model in the case of large aspect ratio.

## 2. Model of the BFEM

### 2.1 Base force

Consider a two-dimensional domain of solid medium, let  $x^\alpha$  ( $\alpha=1,2$ ) denote the Lagrangian coordinate system. In order to describe the stress state at a point  $Q$ , a parallelogram with the edges  $dx^1e_1$ ,  $dx^2e_2$  is shown in Fig. 1, where  $e_1$  and  $e_2$  are unit vectors. Define,

$$t^\alpha = \frac{dT^\alpha}{dx^{\alpha+1}}, \quad dx^\alpha \rightarrow 0 \quad (1)$$

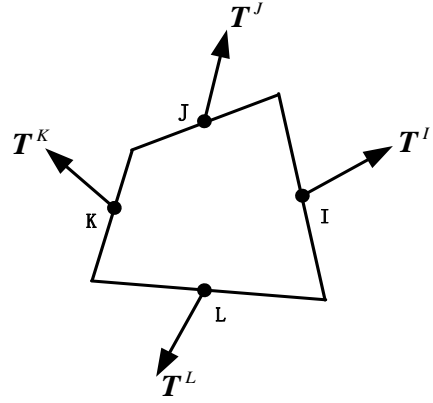


Fig. 3 Four-mid-node plane element

where  $3=1$  for indexes. Quantities  $t^\alpha$  ( $\alpha=1,2$ ) are called the base forces at point  $Q$  in the two-dimensional coordinate system  $x^\alpha$ .

The gradient of displacement  $u_\alpha$  can be written as

$$u_\alpha = \frac{\partial u}{\partial x^\alpha} \quad (2)$$

### 2.2 A degenerate base force element

In the paper (Peng *et al.*2014b), the compliance matrix of a concave polygonal element with  $n$  nodes as shown in Figure 2 was be reduced as follows:

$$D_{IJ} = \frac{1+\nu}{EA} \left( r_{IJ}U - \frac{\nu}{1+\nu} r_I \otimes r_J \right), \quad (I, J = 1, 2, 3, \dots, n) \quad (3)$$

where  $E$  is Young's modulus,  $\nu$  is Poisson's ratio,  $A$  is the original area of the element,  $r_{IJ}$  is the dot product of position vectors  $r_I$  and  $r_J$  of points  $I$  and  $J$ ,  $U$  is the unit vectors which can be written as

$$U = e_1 \otimes e_1 + e_2 \otimes e_2 \quad (4)$$

In this paper, we consider a 4-mid-node plane element as shown in Fig. 3. Let  $I, J, K, L$  denote its sides, and  $T^I, T^J, T^K, T^L$  the force vectors acting on each of the sides.

We found that the compliance matrix of the concave polygonal element can be degenerated into a four-mid-node plane element. The compliance matrix of the degenerate base force element can be written as follow:

$$D_{IJ} = \frac{1+\nu}{EA} \left( r_{IJ}U - \frac{\nu}{1+\nu} r_I \otimes r_J \right), \quad (I, J = 1, 2, 3, 4) \quad (5)$$

in which

$$\left. \begin{aligned} r_I &= r_{I1}e_1 + r_{I2}e_2 \\ r_J &= r_{J1}e_1 + r_{J2}e_2 \end{aligned} \right\} \quad (6)$$

The compliance matrix of these two kinds of elements are the same. Further, the compliance matrix of an element can be written as follow

$$\mathbf{D}_{IJ} = \frac{1+\nu}{EA} \begin{bmatrix} \frac{1}{1+\nu} r_{I1} r_{J1} + r_{I2} r_{J2} & -\frac{\nu}{1+\nu} r_{I1} r_{J2} \\ -\frac{\nu}{1+\nu} r_{I2} r_{J1} & r_{I1} r_{J1} + \frac{1}{1+\nu} r_{I2} r_{J2} \end{bmatrix} \quad (7)$$

( $I, J = 1, 2, 3, 4$ )

For a plane strain problem, it is necessary to replace  $E$  by  $E/(1-\nu^2)$  and  $\nu$  by  $\nu/(1-\nu)$  in Eqs. (5), (7).

In the above derivation, the following equilibrium conditions were used

$$\left. \begin{array}{l} \sum_I \mathbf{T}^I = 0 \\ \mathbf{T}^I \times \mathbf{r}_I = 0 \end{array} \right\} \quad (8)$$

Now, we can release the equilibrium condition of an element using the Lagrange multiplier method as follow

$$\Pi_C^* (\mathbf{T}, \boldsymbol{\lambda}_M, \lambda_N) = W_C^e + \boldsymbol{\lambda}_M \left( \sum_I \mathbf{T}^I \right) + \lambda_N (\mathbf{T}^I \times \mathbf{r}_I) \quad (9)$$

in which, arbitrary vectors  $\boldsymbol{\lambda}_M = \{\lambda_1 \lambda_2\}$  and  $\boldsymbol{\lambda}_M$  is the Lagrange multipliers,  $W_C^e$  is the complementary energy of the degenerate base force element,  $\Pi_C^* (\mathbf{T}, \boldsymbol{\lambda}_M, \lambda_N)$  is new energy function of the degenerate element.

The complementary energy of a degenerate element for an isotropic material can be written as

$$W_C^e = \frac{1+\nu}{2EA} \left[ (\mathbf{T}^I \cdot \mathbf{T}^J) r_{IJ} - \frac{\nu}{1+\nu} (\mathbf{T}^I \cdot \mathbf{r}_I)^2 \right] \quad (10)$$

( $I, J = 1, 2, 3, 4$ )

in which

$$\left. \begin{array}{l} \mathbf{T}^I = T^{I1} \mathbf{e}_1 + T^{I2} \mathbf{e}_2 \\ \mathbf{T}^J = T^{J1} \mathbf{e}_1 + T^{J2} \mathbf{e}_2 \end{array} \right\} \quad (11)$$

The new complementary energy function of the elastic system with  $n$  elements can be written as

$$\Pi_C^* = \sum_n \Pi_C^{e*} \quad (12)$$

And by means of modified complementary energy principle, we can obtain the control equation of elastic system

$$\left\{ \begin{array}{l} \frac{\partial \Pi_C^* (\mathbf{T}, \boldsymbol{\lambda}_M, \lambda_N)}{\partial \mathbf{T}} = 0 \\ \frac{\partial \Pi_C^* (\mathbf{T}, \boldsymbol{\lambda}_M, \lambda_N)}{\partial \boldsymbol{\lambda}_M} = 0 \\ \frac{\partial \Pi_C^* (\mathbf{T}, \boldsymbol{\lambda}_M, \lambda_N)}{\partial \lambda_N} = 0 \end{array} \right. \quad (13)$$

**2.3 Explicit expression for the stress of element and the displacement of node**

Now, the explicit expression of displacement can be obtained as

$$\boldsymbol{\delta}_I = \frac{\partial \Pi_C^* (\mathbf{T}, \boldsymbol{\lambda}_M, \lambda_N)}{\partial \mathbf{T}^I} \quad (14)$$

Further, the displacement vectors of an element can be reduced as follows

$$\begin{aligned} \boldsymbol{\delta}_I &= (\mathbf{D}_{I1J1} T^{J1} + \mathbf{D}_{I1J2} T^{J2} + \lambda_1 + \lambda_N \mathbf{r}_{I2}) \mathbf{e}_1 \\ &+ (\mathbf{D}_{I2J1} T^{J1} + \mathbf{D}_{I2J2} T^{J2} + \lambda_2 - \lambda_N \mathbf{r}_{I1}) \mathbf{e}_2 \end{aligned} \quad (15)$$

And the explicit expression of stress for the 4-mid-node element can be written as

$$\begin{aligned} \boldsymbol{\sigma} &= \frac{1}{A} \sum_{I=1}^4 \left[ T^{I1} r_{I1} \mathbf{e}_1 \otimes \mathbf{e}_1 + T^{I1} r_{I2} \mathbf{e}_1 \otimes \mathbf{e}_2 \right. \\ &\left. + T^{I2} r_{I1} \mathbf{e}_2 \otimes \mathbf{e}_1 + T^{I2} r_{I2} \mathbf{e}_2 \otimes \mathbf{e}_2 \right] \end{aligned} \quad (16)$$

### 3. Flow chart of the BFEM

According to the above derivation, we make out the program of the BFEM based on the complementary energy principle can be shown in Fig. 4.

The differences between the present method and the conventional finite element method of complementary energy principle are as follow:

(1) The traditional finite element method of complementary energy principle is usually constructing the stress interpolation function of an element first, and then constructing the compliance matrix of an element. However, the choice of interpolation function is very difficult. Because the interpolation function is not only to ensure that the stress can balance in each element, but also to ensure that the stress can balance in the junction of each element and the stress boundary of an element. It is difficult to find out the further breakthrough of the finite element method of complementary energy principle under the framework of this kind of solution. The present method does not need to construct the compliance matrix of an element using stress interpolation function.

(2) The conventional finite element method of complementary energy principle needs to use the Gauss integral method to calculate the compliance matrix of an element. However, the compliance matrix of the present method is an explicit expression which does not use the numerical integration. So the calculation accuracy and operation speed are improved.

(3) The conventional finite element method of complementary energy principle is usually using quadrilateral elements for plane problems. But the base force element method can use either quadrilateral elements or arbitrary polygonal elements. The base force element method is not restricted by the shape of the element. And the expression of compliance matrix of the base force element method is a unified mathematical expression. Its programming calculation is very simple.

(4) In a conventional finite element method of

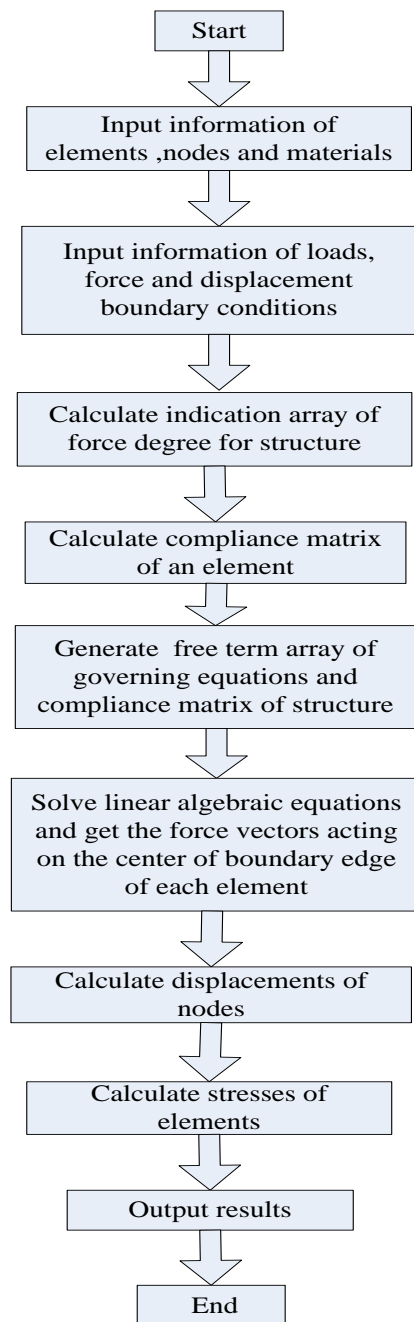


Fig. 4 Flow chart of main program of the BFEM

complementary energy principle, the displacement is difficult to solve. The displacement is solved using integral method by the geometric equation after the element strain is obtained. The method of using the base force element method to calculate the node displacement is very simple. In the present method, the displacement of nodes can be calculated directly by using the governing equations of elements. It does not need to be integral, thus it can ensure the accuracy of the present method.

(5) The base force element method uses the base force vector to express the stress state and uses the displacement gradient to describe the state of

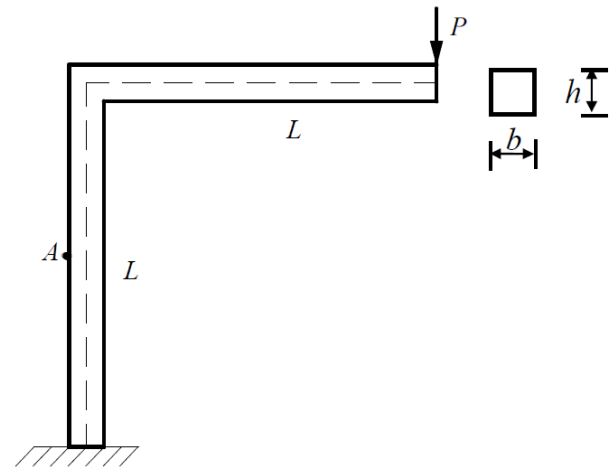


Fig. 5 A right angle cantilever frame loaded by a concentrated end load

deformation. This shows its superiority in the derivation of formula and the expression of mathematics. So it has good application prospects.

#### 4. Numerical examples

The present formulation of base force element method will be used for the linear elastic analysis of plane frame structure in this section. The numerical experiments are performed in order to establish the validity and accuracy of the base force element method, as well as to assess the relative performance of the present elements. The results obtained from present developments are compared with corresponding analytical solutions. The responses obtained using the standard displacement method are also given for some problems in order to assess the potential advantages of the base force element method. All displacement method calculations are performed using the four-node isoparametric element (Q4 model).

Example-1: Consider a rectangular cantilever frame under concentrated force shown in Fig. 5. The cantilever frame has the length  $L=10$  m, height  $h=1$  m, width  $b=1$  m, elastic modulus  $E=1 \times 10^8$  Pa and Poisson's ratio  $\nu=0$ . While the applied load is  $P=1$  N. The theoretical solution of deflection at free end of the cantilever frame is  $1.6 \times 10^{-8}$  m.

The calculated specimen was divided into the 4-mid-node base force elements with the center nodes of each of the sides. In order to consider the influence of the aspect ratio of element, we adopt three kinds of element meshes as shown in Fig. 6, successively.

The values of deflection at free end of the cantilever frame are compared with those provided by the theoretical solution, conventional quadrilateral isoparametric element (Q4 model) and quadrilateral reduced integration element (Q4R model) in Table 1, Fig. 7, respectively. The results show that the predicted response using the two-dimensional quadrilateral isoparametric element (Q4 element) deviates from the theoretical solution with large element aspect ratios and the 4-mid-node element of BFEM has very good performance compared with Q4 model and Q4R model.

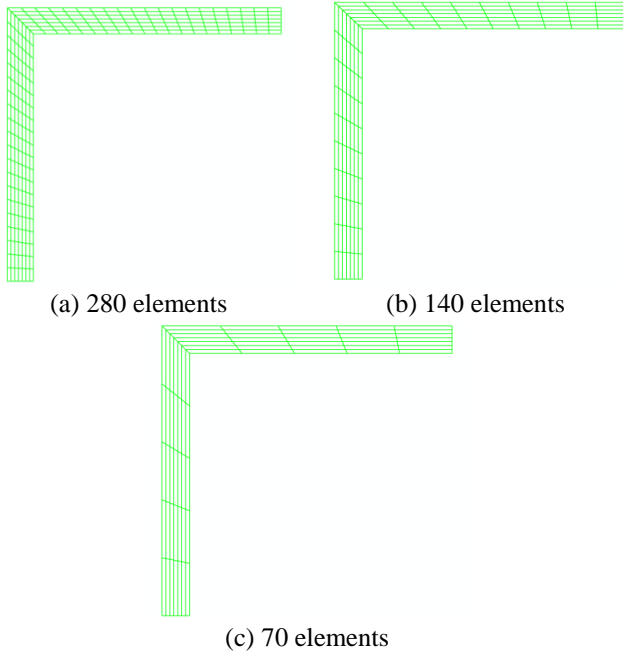


Fig. 6 Three element meshes with different aspect ratios

Table 1 Vertical displacement of the right-angle cantilever frame

Mesher	Theoretical ( $\times 10^{-4}$ m)	BFEM ( $\times 10^{-4}$ m)	Q4 model ( $\times 10^{-4}$ m)	Q4R model ( $\times 10^{-4}$ m)
7×40	-1.6000	-1.6100	-1.2525	-1.6031
7×20	-1.6000	-1.6042	-0.8317	-1.5911
7×10	-1.6000	-1.5941	-0.3634	-1.5453

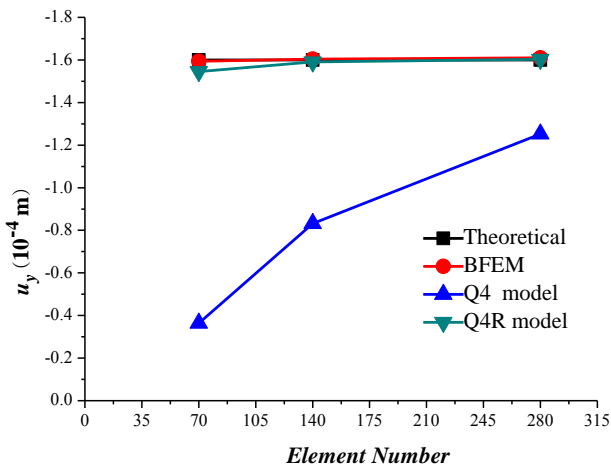


Fig. 7 Relation curves of the number of mesh elements and free end vertical displacement

The  $\sigma_y$  of the point A of the cantilever frame with different meshes are listed in Table 2, Fig. 8, respectively. The numerical results of the present model are consistent with those of Q4R model and the 4-mid-node element of BFEM has very good performance compared with Q4 model for large aspect ratio of element.

Example-2: Consider a rectangular cantilever frame under a tip moment shown in Fig. 9. The cantilever frame has the length  $L=15$  m, height  $h=1$  m, width  $b=1$  m,

Table 2 The  $\sigma_y$  of the point A of the right-angle frame loaded by a concentrated load

Mesher	BFEM(Pa)	Q4 model (Pa)	Q4R model (Pa)
7×40	51.5021	41.7433	51.4775
7×20	52.1003	27.9487	51.9031
7×10	47.9929	11.7328	48.2981

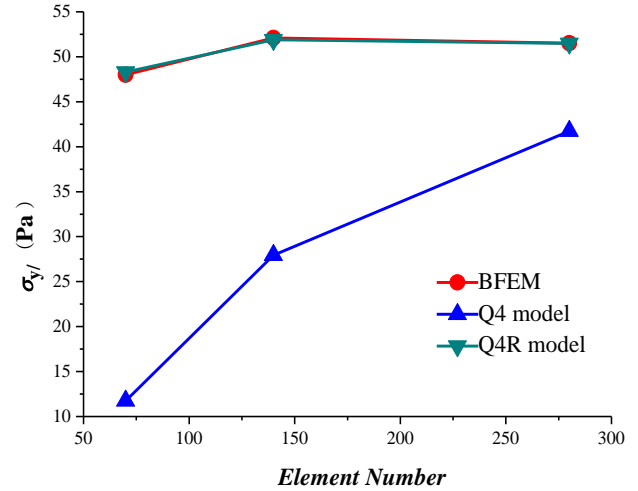


Fig. 8 Relation curves of the number of mesh elements and the  $\sigma_y$  of the point A

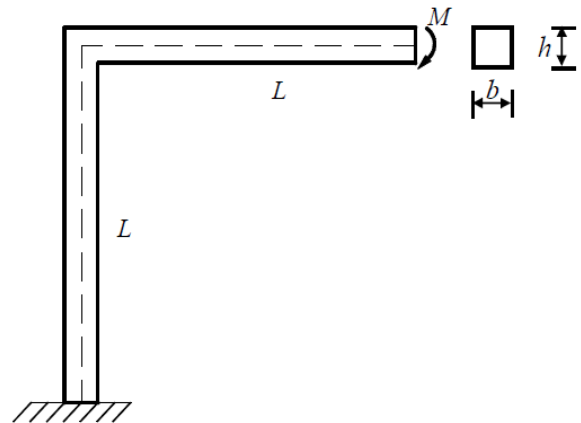


Fig. 9 A right angle cantilever frame loaded by a tip moment

Poisson's ratio  $\nu=0$  and elastic modulus  $E=1 \times 10^7$  Pa. While the tip moment is  $M=1000$  N·m. The theoretical solution of deflection at free end of the cantilever frame is  $4.050 \times 10^{-6}$  m.

The calculated specimen was divided into the 4-mid-node base force elements with the center nodes of each of the sides. In order to consider the influence of the aspect ratio of element, we adopt four kinds of element meshes as shown in Fig. 10, successively.

The values of deflection at free end of the cantilever frame are compared with those provided by the theoretical solution, conventional quadrilateral isoparametric element (Q4 model) and quadrilateral reduced integration element (Q4R model) in Table 3, Fig. 11, respectively. The results show that the predicted response using the 4-node two-dimensional isoparametric element (Q4 element) deviates

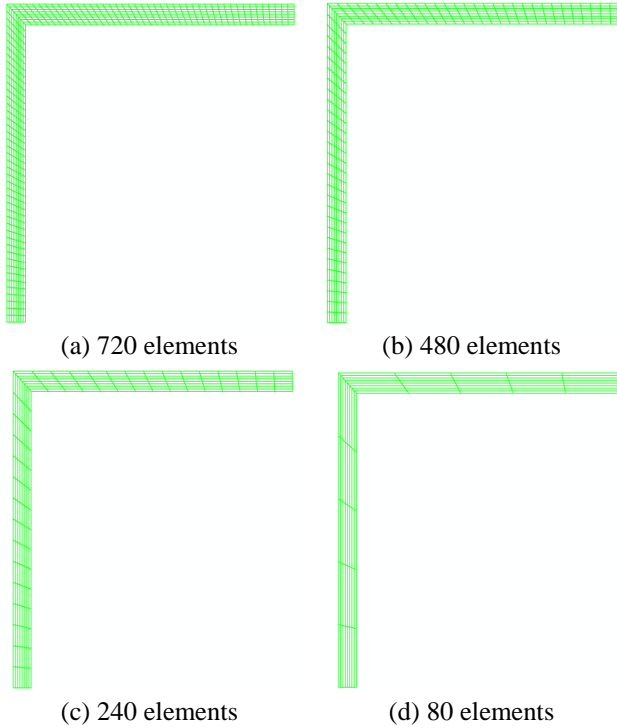


Fig. 10 Four kinds of element meshes with different aspect ratios

Table 3 Vertical displacement of the right-angle cantilever frame loaded by a tip moment

Meshes	Theoretical ( $\times 10^{-6}$ m)	BFEM ( $\times 10^{-6}$ m)	Q4 model ( $\times 10^{-6}$ m)	Q4R model ( $\times 10^{-6}$ m)
8 $\times$ 90	-4.0500	-4.0154	-3.5756	-4.0693
8 $\times$ 60	-4.0500	-4.0120	-3.2265	-4.0659
8 $\times$ 30	-4.0500	-4.0059	-2.1448	-4.0495
8 $\times$ 10	-4.0500	-3.9778	-0.4849	-3.8900

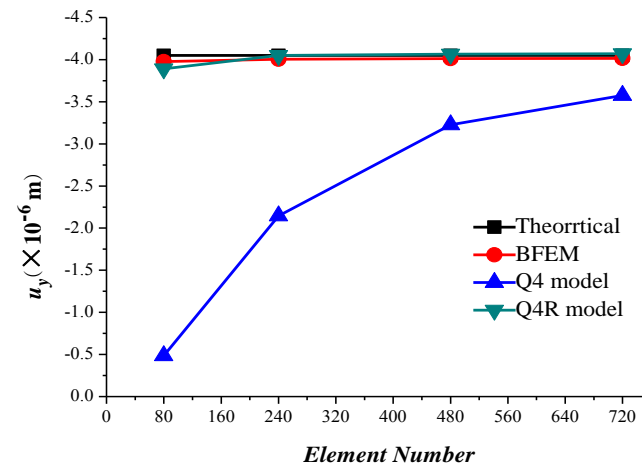


Fig. 11 Relation curves of the number of mesh elements and free end vertical displacement

from the theoretical solution with large element aspect ratios and the 4-mid-node element of BFEM has very good performance compared with Q4 model and Q4R model.

The  $\sigma_x$  of each element at free end of the cantilever

Table 4 The  $\sigma_x$  of the center of each element at the right of right-angle cantilever frame

y (m)	BFEM (Pa)	Q4 model (Pa)	Q4R model (Pa)
15.4375	5250.4266	4974.6000	5326.4000
15.3125	3750.5686	3555.9800	3809.3300
15.1875	2249.7926	2136.0100	2287.4500
15.0625	750.2947	715.4660	764.4880
14.9375	-749.8102	-705.4640	-758.6870
14.8125	-2250.7960	-2126.8300	-2283.1200
14.6875	-3749.7322	-3548.9400	-3807.7700
14.5625	-5249.9319	-4972.7900	-5337.9800

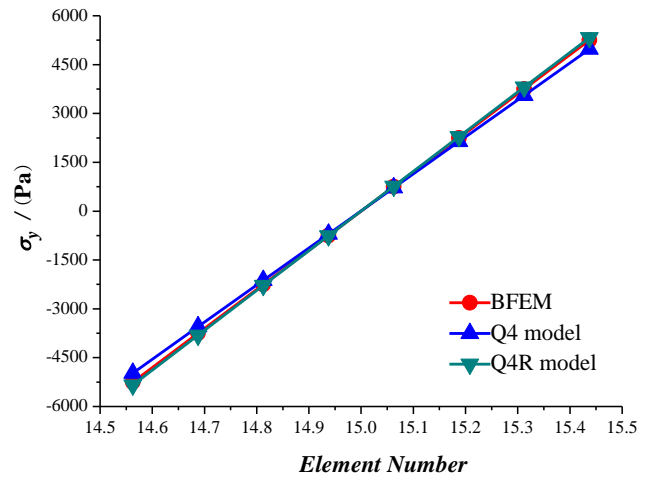


Fig. 12  $y$ - $\sigma_x$  curves of the center of each cell at the right of right-angle cantilever frame

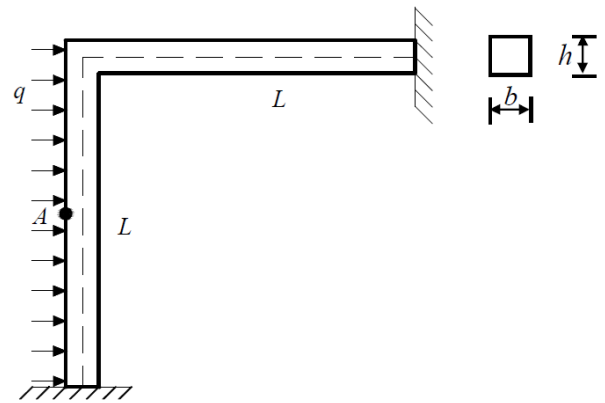


Fig. 13 Right-angle frame under uniformly distributed load

frame with different meshes are listed in Table 4, Fig. 12, respectively. The numerical results of the present model are consistent with those of Q4R model and the 4-mid-node element of BFEM has very good performance compared with Q4 model for large aspect ratio of element.

Example-3: Consider a rectangular cantilever frame under uniformly distributed load shown in Fig. 13. The cantilever frame has the length  $L=15$  m, height  $h=1$  m, width  $b=1$  m, elastic modulus  $E=1 \times 10^6$  Pa and Poisson's ratio  $\nu=0$ . While the uniformly distributed load is  $q=1000$  N/m. The theoretical solution of horizontal displacement of the point A of the cantilever frame is  $4.1092 \times 10^{-5}$  m.

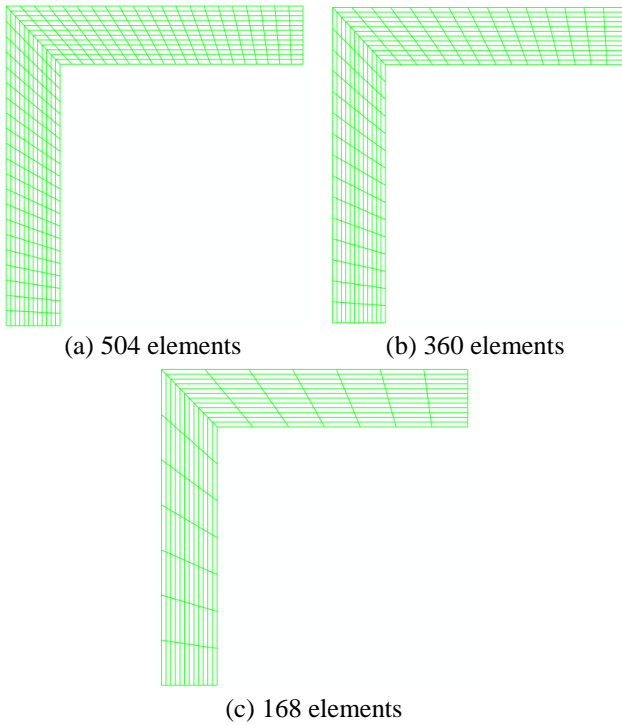


Fig. 14 Three element meshes with different aspect ratios

Table 5 Horizontal displacement of the point A of the right-angle frame

Meshes	Theoretical ( $\times 10^{-5}$ m)	BFEM ( $\times 10^{-5}$ m)	Q4 model ( $\times 10^{-5}$ m)	Q4R model ( $\times 10^{-5}$ m)
12 $\times$ 42	4.1092	4.0904	3.8729	4.0789
12 $\times$ 30	4.1092	4.0556	3.7213	4.0445
12 $\times$ 14	4.1092	3.7416	2.9475	3.7954

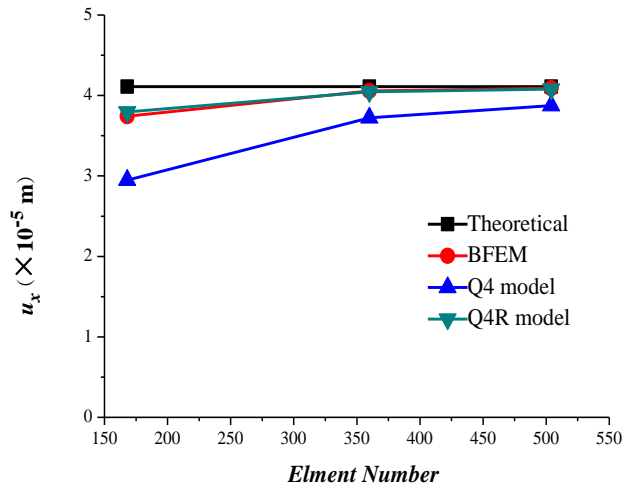


Fig. 15 Relation curves of the number of mesh elements and horizontal displacement of the point A

The calculated specimen was divided into the 4-mid-node base force elements with the center nodes of each of the sides. In order to consider the influence of the aspect ratio of element, we adopt three kinds of element meshes as shown in Fig. 14, successively.

The values of horizontal displacement of the point A of

Table 6 The  $\sigma_y$  of the point of A of right-angle cantilever frame

Meshes	BFEM(Pa)	Q4 model (Pa)	Q4R model (Pa)
12 $\times$ 42	-7445.53	-6984.15	-7444.02
12 $\times$ 30	-7420.10	-6823.23	-7410.46
12 $\times$ 14	-7593.09	-5166.12	-7808.32

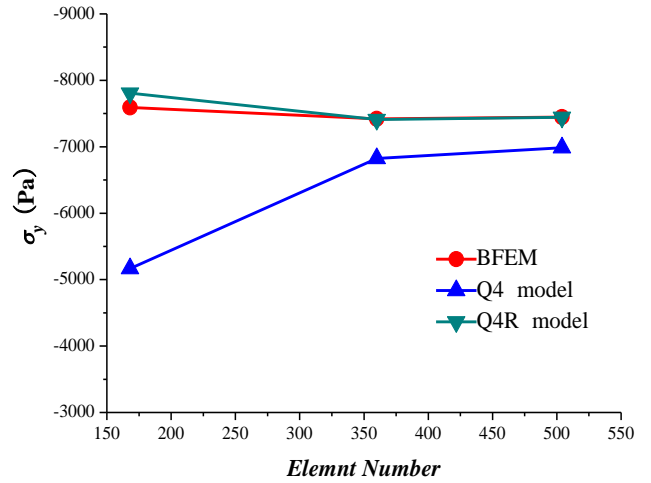


Fig. 16 Relation curves of the number of mesh elements and the  $\sigma_y$  of the point A

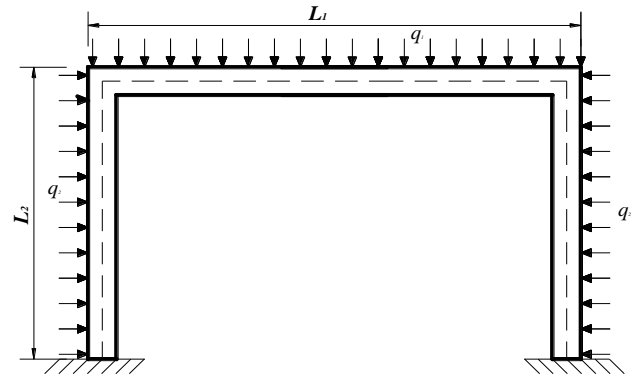


Fig. 17 The frame under uniformly distributed load

the cantilever frame are compared with those provided by the theoretical solution, conventional quadrilateral isoparametric element (Q4 model) and quadrilateral reduced integration element (Q4R model) in Table 5, Fig. 15, respectively. The results show that the predicted response using the 4-node two-dimensional isoparametric element (Q4 element) deviates from the theoretical solution with large element aspect ratios and the 4-mid-node element of BFEM has very good performance compared with Q4 model and Q4R model.

The  $\sigma_y$  of the point A of the cantilever frame with different meshes are listed in Table 6, Fig. 16, respectively. The numerical results of the present model are consistent with those of Q4R model and the 4-mid-node element of BFEM has very good performance compared with Q4 model for large aspect ratio of element.

Example-4: Consider a frame under uniformly distributed load shown in Fig. 17. The frame has the length

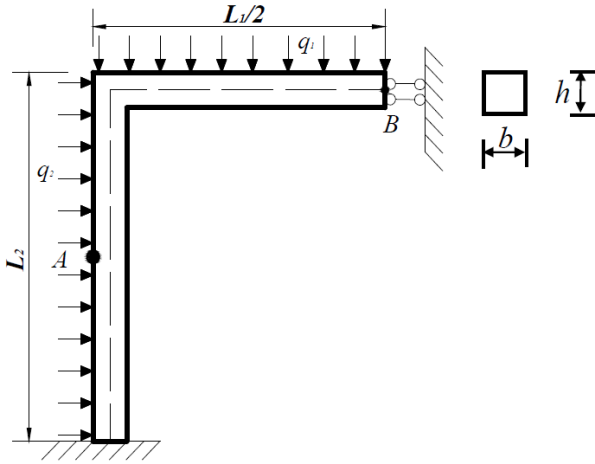


Fig. 18 1/2 structure of the frame

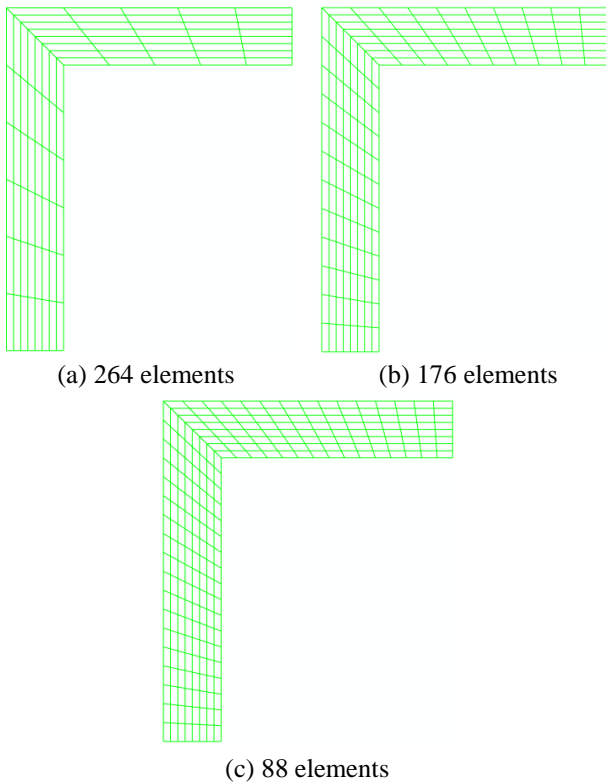


Fig. 19 Three element meshes with different aspect ratios

$L_1=10$  m,  $L_2=6$  m, height  $h=1$  m, width  $b=1$  m, elastic modulus  $E=2 \times 10^7$  Pa and Poisson's ratio  $\nu=0$ . While the uniformly distributed load is  $q_1=100$  N/m,  $q_2=200$  N/m. The theoretical solution of horizontal displacement of the point A of the cantilever frame is  $4.1092 \times 10^{-5}$  m, and vertical displacement of the point B is  $13.3112 \times 10^{-4}$  m ( Santos and Almeida 2010).

Symmetry of the axial and loading will be considered. Such that only 1/2 of the domain needs to be considered, as shown in Fig. 18.

The calculated specimen was divided into the 4-mid-node base force elements with the center nodes of each of the sides. In order to consider the influence of the aspect ratio of element, we adopt three kinds of element meshes as

Table 7 Horizontal displacement of the point A of the frame under uniformly distributed load

Meshes	Theoretical ( $\times 10^{-4}$ m)	BFEM ( $\times 10^{-4}$ m)	Q4 model ( $\times 10^{-4}$ m)	Q4R model ( $\times 10^{-4}$ m)
8×33	3.0385	3.0422	2.7739	3.0355
8×22	3.0385	3.0072	2.5828	2.9952
8×11	3.0385	2.7662	1.9789	2.7298

Table 8 Vertical displacement of the point A of the frame under uniformly distributed load

Meshes	Theoretical ( $\times 10^{-4}$ m)	BFEM ( $\times 10^{-4}$ m)	Q4 model ( $\times 10^{-4}$ m)	Q4R model ( $\times 10^{-4}$ m)
8×33	-13.3112	13.3958	-11.2972	-13.3176
8×22	-13.3112	-13.1637	-10.2687	-13.1520
8×11	-13.3112	-12.4735	-7.4196	-12.6871

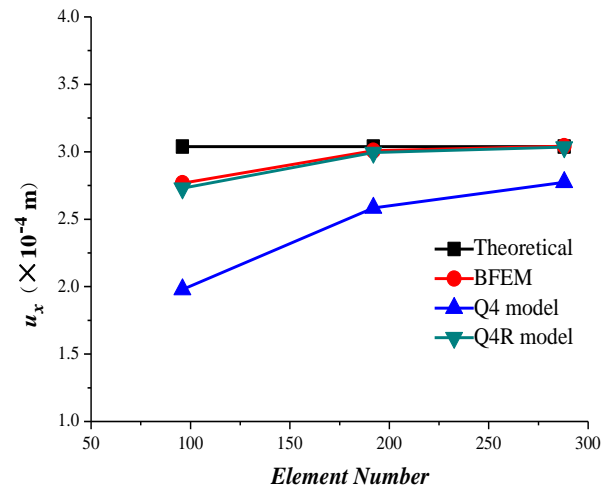


Fig. 20 Relation curves of the number of mesh elements and horizontal displacement of the point A

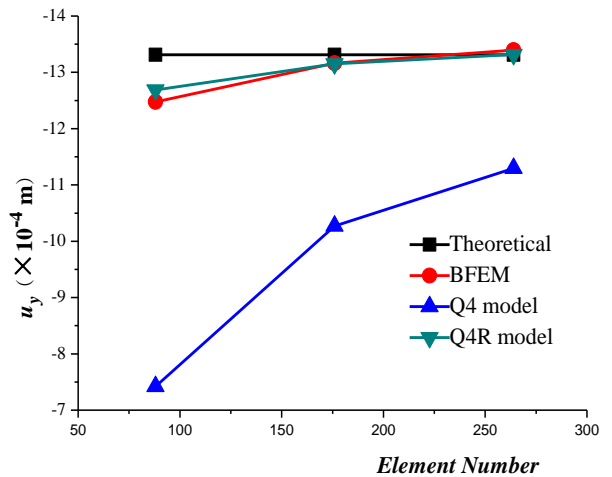


Fig. 21 Relation curves of the number of mesh elements and vertical displacement of the point B

shown in Fig. 19, successively.

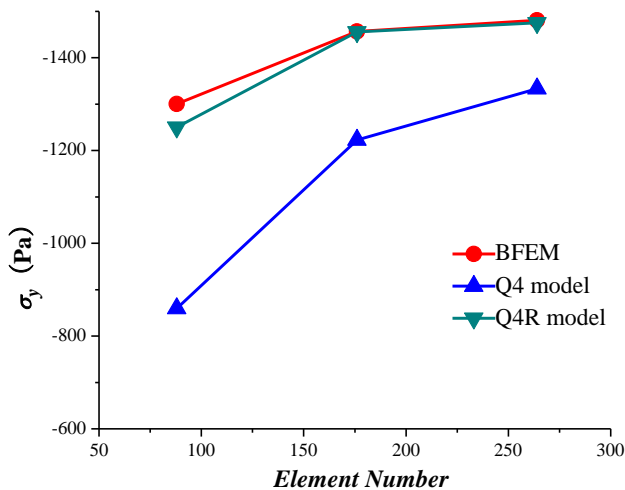
The values of horizontal displacement of the point A and vertical displacement of the point B of the frame are compared with those provided by the theoretical solution,

Table 9 The  $\sigma_y$  of the point of A of the frame

Meshes	BFEM(Pa)	Q4 model(Pa)	Q4R model (Pa)
8×33	-1300.66	-859.73	-1286.23
8×22	-1456.59	-1222.81	-1455.69
8×11	-1480.78	-1333.38	-1475.45

Table 10 The  $\sigma_x$  of the point of B of the frame

Unite Number	BFEM(Pa)	Q4(Pa)	Q4R(Pa)
8×33	-691.96	-702.31	-692.18
8×22	-691.75	-721.74	-692.09
8×11	-716.27	-725.67	-716.02

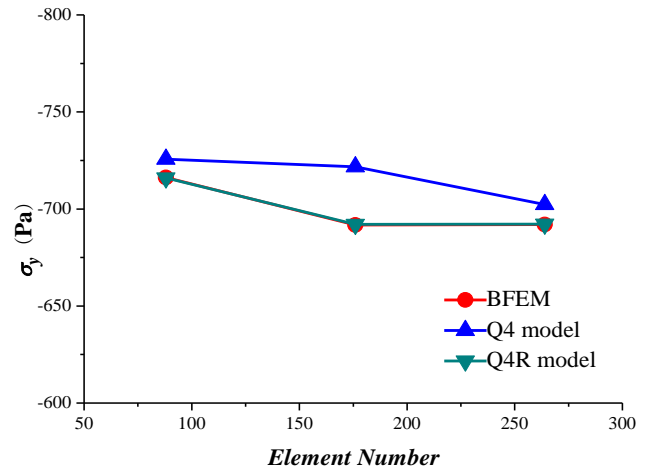
Fig. 22 Relation curves of the number of mesh elements and the  $\sigma_y$  of the point A

conventional quadrilateral isoparametric element (Q4 model) and quadrilateral reduced integration element (Q4R model) in Tables 7-8, Figs. 20,21, respectively. The results show that the predicted response using the two-dimensional quadrilateral isoparametric element (Q4 element) deviates from the theoretical solution with large element aspect ratios and the 4-mid-node element of BFEM has very good performance compared with Q4 model and Q4R model.

The  $\sigma_y$  of the point A and the  $\sigma_x$  of the point of B of frame with different meshes are listed in Tables 9-10, Figs. 22, 23, respectively. The numerical results of the present model are consistent with those of Q4R model and the 4-mid-node element of BFEM has very good performance compared with Q4 model for large aspect ratio of element.

## 5. Conclusions

In this paper, a degenerated 4-mid-node plane element from concave polygonal element of BFEM was presented. The application of base force element method on complementary energy principle is used to analyze the plane frame structure. Based on the complementary energy principle, the equilibrium conditions are released by Lagrange multiplier method, and a modified complementary energy principle described by the base force is obtained. A new BFEM procedure is developed using

Fig. 23 Relation curves of the number of mesh elements and the  $\sigma_x$  of the point B

MATLAB language. The chief features of the method are that the model does not introduce an interpolating function and can be used in any coordinate system, and is not necessary to introduce the Gauss` integral for calculating the compliance coefficient at a point.

The calculation results of BFEM on complementary energy principle coincide with the theoretical solution and quadrilateral reduced integration element (Q4R model). The correctness of the present method and its computer program is verified. And the researches show that it has a very good performance for large aspect ratio of element. The plane frame structure is solved by base force element method, and further research results on large deformation will be published in the future. The advantages of the BFEM are simple and effective, and it has widely application extension.

## Acknowledgements

This work is supported by National Science Foundation of China (10972015, 11172015), Beijing Natural Science Foundation (8162008) and Pre-exploration Project of Key Laboratory of Urban Security and Disaster Engineering, Ministry of Education, Beijing University of Technology (USDE201404).

## References

- Cen, S., Fu, X.R. and Zhou, M.J.(2011), "8- and 12-node plane hybrid stress-function elements immune to severely distorted mesh containing elements with concave shapes", *Comput. Meth. Appl. Mech. Eng.*, **200**(29-32), 2321-2336.
- Cen, S., Fu, X.R., Zhou, G.H., Zhou, M.J. and Li, C.F. (2011), "Shape-free finite element method: The plane Hybrid Stress-Function (HS-F) element method for anisotropic materials", *Sci. China Phys. Mech. Astron.*, **54**(4), 653-665.
- Cen, S., Zhou, M.J. and Fu, X.R. (2011), "A 4-node hybrid stress-function (HS-F) plane element with drilling degrees of freedom less sensitive to severe mesh distortions", *Comput. Struct.*, **89**(5-6), 517-528.

- Chen, J., Li, C.J. and Chen, W.J. (2010), "A family of spline finite elements", *Comput. Struct.*, **88**(11-12), 718-727.
- Darilmaz, K. (2005), "An assumed-stress finite element for static and free vibration analysis of Reissner-Mindlin plates", *Struct. Eng. Mech.*, **19**(2), 199-215.
- De Veubeke, B.F. (1965), "Displacement and equilibrium models in the finite element method", *Stress Anal.*, **9**, 145-197.
- de Veubeke, B.F. (1972), "A new variational principle for finite elastic displacements", *Int. J. Eng. Sci.*, **10**(9), 745-763.
- Fu, X.R., Cen, S., Li, C.F. and Chen, X.M. (2010), "Analytical trial function method for development of new 8-node plane element based on the variational principle containing airy stress function", *Eng. Comput.*, **27**(4), 442-463.
- Gao, Y.C. (2003), "A new description of the stress state at a point with applications", *Arch. Appl. Mech.*, **73**(3-4), 171-183.
- Hughes, T.J.R. (1980), "Generalization of selective integration procedures to anisotropic and nonlinear media", *Int. J. Numer. Meth. Eng.*, **15**(9), 1413-1418.
- Liu, G.R., Dai, K.Y. and Nguyen, T.T. (2007), "A smoothed finite element method for mechanics problems", *Comput. Mech.*, **39**(6), 859-877.
- Liu, G.R., Nguyen-Thoi, T. and Lam, K.Y. (2008), "A novel alpha finite element method ( $\alpha$ FEM) for exact solution to mechanics problems using triangular and tetrahedral elements", *Comput. Meth. Appl. Mech. Eng.*, **197**(45-48), 3883-3897.
- Liu, Y.H., Peng, Y.J., Zhang, L.J. and Guo, Q. (2013), "A 4-mode-node plane model of base force element method on complement energy principle", *Math. Prob. Eng.*, **2013**, 1-8.
- Long, Y.Q. and Huang, M.F. (1988), "A generalized conforming isoparametric element", *Appl. Math. Mech.*, **9**(10), 929-936.
- Long, Y.Q., Cen, S. and Long, Z.F. (2009), *Advanced Finite Element Method in Structural Engineering*, Springer-Verlag GmbH/Tsinghua University Press, Berlin, Heidelberg/Beijing.
- Long, Y.Q., Li, J.X., Long, Z.F. and Cen, S. (1999), "Area coordinates used in quadrilateral elements", *Commun. Numer. Meth. Eng.*, **15**(8), 533-545.
- Long, Z.F., Cen, S., Wang, L., Fu, X.R. and Long, Y.Q. (2010), "The third form of the quadrilateral area coordinate method (QACM-III): theory, application, and scheme of composite coordinate interpolation", *Finite Elem. Anal. Des.*, **46**(10), 805-818.
- Long, Z.F., Li, J.X., Cen, S. and Long, Y.Q. (1999), "Some basic formulae for area coordinates used in quadrilateral elements", *Commun. Numer. Meth. Eng.*, **15**(12), 841-852.
- Moes, N., Dolbow, J. and Belytschko, T. (1999), "A finite element method for crack growth without remeshing", *Int. J. Numer. Meth. Eng.*, **46**(1), 131-150.
- Patnaik, S.N. (1973), "An integrated force method for discrete analysis", *Int. J. Numer. Meth. Eng.*, **6**(2), 237-251.
- Patnaik, S.N. (1986), "The integrated force method versus the standard force method", *Comput. Struct.*, **22**(2), 151-163.
- Patnaik, S.N. (1986), "The variational energy formulation for the integrated force method", *AIAA J.*, **24**(1), 129-136.
- Patnaik, S.N., Berke, L. and Gallagher, R.H. (1991), "Integrated force method versus displacement method for finite element analysis", *Comput. Struct.*, **38**(4), 377-407.
- Peng, Y.J. and Liu, Y.H. (2009), "Base force element method (BFEM) of complementary energy principle for large rotation problems", *Acta Mechanica Sinica*, **25**(4), 507-515.
- Peng, Y.J., Dong, Z.L., Peng, B. and Liu, Y.H. (2011), "Base force element method (BFEM) on potential energy principle for elasticity problems", *Int. J. Mech. Mech. Des.*, **7**(3), 245-251.
- Peng, Y.J., Guo, Q., Zhang, Z.F. and Shan, Y.Y. (2015), "Application of base force element method on complement energy principle to rock mechanics problems", *Math. Prob. Eng.*, **25**(4), 1-16.
- Peng, Y.J., Zhang, L.J., Pu, J.W. and Guo, Q. (2014), "A two-dimensional base force element method using concave polygonal mesh", *Eng. Anal. Bound. Elem.*, **42**, 45-50.
- Peng, Y.J., Zong, N.N., Zhang, L.J. and Pu, J.W. (2014), "Application of 2D base force element method with complementary energy principle for arbitrary meshes", *Eng. Comput.*, **31**(4), 1-15.
- Pian, T.H.H. (1964), "Derivation of element stiffness matrices by assumed stress distributions", *AIAA J.*, **2**(7), 1333-1336.
- Pian, T.H.H. and Chen, D.P. (1982), "Alternative ways for formulation of hybrid stress elements", *Int. J. Numer. Meth. Eng.*, **18**(11), 1679-1684.
- Pian, T.H.H. and Sumihara, K. (1984), "Rational approach for assumed stress finite elements", *Int. J. Numer. Meth. Eng.*, **20**(9), 1685-1695.
- Piltner, R. and Taylor, R.L. (1995), "A quadrilateral mixed finite element with two enhanced strain modes", *Int. J. Numer. Meth. Eng.*, **38**(11), 1783-1808.
- Rajendran, S. and Liew, K.M. (2003), "A novel unsymmetric 8-node plane element immune to mesh distortion under a quadratic displacement field", *Int. J. Numer. Meth. Eng.*, **58**(11), 1713-1748.
- Santos, H.A.F.A. and Paulo, C.A. (2011), "On a pure complementary energy principle and a force-based finite element formulation for nonlinear elastic cables", *Int. J. Nonlin. Mech.*, **46**(2), 395-406.
- Santos, H.A.F.A. (2011), "Complementary-energy methods for geometrically non-linear structural models: an overview and recent developments in the analysis of frames", *Arch. Comput. Meth. Eng.*, **18**(4), 405-440.
- Santos, H.A.F.A. (2015), "A novel updated Lagrangian complementary energy-based formulation for the elastica problem: force-based finite element model", *Acta Mechanica*, **226**(4), 1133-1151.
- Santos, H.A.F.A. and Moitinho de Almeida, J.P. (2010), "Equilibrium-based finite element formulation for the geometrically exact analysis of planar framed structures", *J. Eng. Mech.*, **136**(12), 1474-1490.
- Santos, H.A.F.A. and Moitinho de Almeida, J.P. (2014), "A family of Piola-Kirchhoff hybrid stress finite elements for two-dimensional linear elasticity", *Finite Elem. Anal. Des.*, **85**, 33-49.
- Simo J.C. and Hughes, T.J.R. (1986), "On the variational foundations of assumed strain methods", *J. Appl. Mech.*, **53**(1), 51-54.
- Tang, L.M., Chen, W.J. and Liu, Y.G. (1984), "Formulation of quasi-conforming element and Hu-Washizu principle", *Comput. Struct.*, **19**(1-2), 247-250.
- Wilson E.L., Taylor R.L., Doherty W.P. and Ghaboussi J. (1973), *Incompatible Displacement Models, Numerical and Computational Methods in Structural Mechanics*, Eds. Fenves, S.J. et al., Academic Press, New York.
- Zhang, C.H., Wang, D.D., Zhang, J.L., Feng, W. and Huang, Q. (2007), "On the equivalence of various hybrid finite elements and a new orthogonalization method for explicit element stiffness formulation", *Finite Elem. Anal. Des.*, **43**(4), 321-332.
- Zienkiewicz, R.L. and Taylor, O.C. (1979), "Complementary energy with penalty functions in finite element analysis", *Energy Methods in Finite Element Analysis*, (A 79-53076 24-39), Chichester, Sussex, England, Wiley-Interscience.